Redox Biology 17 (2018) 200–206

Contents lists available at ScienceDirect

Redox Biology

journal homepage: www.elsevier.com/locate/redox

Short communication

The mitochondrial oxidoreductase CHCHD4 is present in a semi-oxidized state in vivo

Alican J. Erdogan[a,1], Muna Ali[a,b,1], Markus Habich[a,1], Silja L. Salscheider[a], Laura Schu[b], Carmelina Petrungaro[a], Luke W. Thomas[c], Margaret Ashcroft[c], Lars I. Leichert[d], Leticia Prates Roma[e], Jan Riemer[a,*]

[a] Department of Chemistry, Institute of Biochemistry, University of Cologne, Zuelpicher Str. 47a, 50674 Cologne, Germany
[b] Department of Biology, Cellular Biochemistry, University of Kaiserslautern, Erwin-Schroedinger-Str. 13, 67663 Kaiserslautern, Germany
[c] Department of Medicine, University of Cambridge, Cambridge Biomedical Campus, Cambridge, UK
[d] Institute for Biochemistry and Pathobiochemistry - Microbial Biochemistry, Ruhr-Universität Bochum, 44797 Bochum, Germany
[e] Biophysics Department, Center for Integrative Physiology and Molecular Medicine, Saarland University, 66421 Homburg, Saar, Germany

ARTICLE INFO

Keywords:
CHCHD4/ALR/disulfide/redox/mitochondria

ABSTRACT

Disulfide formation in the mitochondrial intermembrane space is an essential process catalyzed by a disulfide relay machinery. In mammalian cells, the key enzyme in this machinery is the oxidoreductase CHCHD4/Mia40. Here, we determined the in vivo CHCHD4 redox state, which is the major determinant of its cellular activity. We found that under basal conditions, endogenous CHCHD4 redox state in cultured cells and mouse tissues was predominantly oxidized, however, degrees of oxidation in different tissues varied from 70% to 90% oxidized. To test whether differences in the ratio between CHCHD4 and ALR might explain tissue-specific differences in the CHCHD4 redox state, we determined the molar ratio of both proteins in different mouse tissues. Surprisingly, ALR is superstoichiometric over CHCHD4 in most tissues. However, the levels of CHCHD4 and the ratio of ALR over CHCHD4 appear to correlate only weakly with the redox state, and although ALR is present in super-stoichiometric amounts, it does not lead to fully oxidized CHCHD4.

1. Introduction

The introduction of disulfide bonds in the mitochondrial intermembrane space (IMS) is an essential process [1–3]. A wide variety of processes depends on disulfide formation, including IMS protein import, Ca^{2+} signaling, relocalization of proteins to mitochondria during cellular stress, apoptosis, hypoxia signaling, tissue regeneration, and respiratory chain assembly [4–11]. Besides conserved pathways like IMS protein import, most of these processes are limited to higher eukaryotes and might even be tissue specific. However, most of our mechanistic knowledge on the mitochondrial disulfide relay is derived from work in *Saccharomyces cerevisiae* and there is only limited knowledge on the mammalian machinery for disulfide formation in the IMS.

A dedicated machinery, the mitochondrial disulfide relay, catalyzes IMS disulfide bond formation. This relay consists of the oxidoreductase CHCHD4 (in yeast: Mia40) and the sulfhydryl oxidase augmenter of liver regeneration ALR (also GFER, hsErv1, in yeast: Erv1) [4,5,12,13]. CHCHD4 contains a redox-active cysteine pair (CPC, where C represents cysteine and P proline), which in its oxidized state can introduce disulfide bonds into substrate proteins. Depletion of CHCHD4 results in strongly delayed oxidation kinetics of its substrates in intact cells [14]. Since oxidation is for many CHCHD4 substrates coupled to their IMS import [7,14], the levels of selected disulfide-containing IMS proteins decrease upon CHCHD4 depletion in human tissue culture cells [14–16]. After introducing disulfides into its substrates, CHCHD4 is present in its reduced state and requires ALR for reoxidation. As it is the case for CHCHD4, depletion of ALR delays substrate oxidation however to a lower extent [14]. From ALR electrons are shuttled via cytochrome *c* to complex IV [17,18]. CHCHD4 and ALR can in part replace their yeast counterparts, implying functional homology of the mammalian and yeast pathways at least for the processes that are conserved [19,20].

The redox state of the active site cysteines of an oxidoreductase is a

Abbreviations: DTT, dithiothreitol; GSH, reduced glutathione; IMS, intermembrane space of mitochondria; MTS, mitochondrial targeting sequence; mmPEG, methyl-polyethylene glycol-maleimide; NEM, N-ethylmaleimide; TCA, trichloroacetic acid; TCEP, Tris(2-carboxyethyl)phosphine

* Corresponding author.
E-mail address: jan.riemer@uni-koeln.de (J. Riemer).
[1] Authors contributed equally.

https://doi.org/10.1016/j.redox.2018.03.014
Received 15 March 2018; Accepted 22 March 2018
Available online 24 March 2018

fundamental indicator of its function. For CHCHD4 the redox states of its cysteines are not known. In yeast Mia40 the CPC motif is present in a partially reduced state (ca. 70–80% oxidized, 20–30% reduced) and this redox state is mainly controlled by Erv1 and the IMS glutathione pool [21]. The oxidized form of Mia40 thereby represents the form that mediates oxidative protein folding. Consequently, shifting the redox state of Mia40 to a more reduced state by either Erv1 depletion or glutaredoxin overexpression impairs oxidative protein folding [21,22]. Instead, the reduced portion of Mia40 could serve in principle in disulfide isomerization, which has so far only been demonstrated in vitro [23,24].

In the present study, we investigated the CHCHD4 redox state, and CHCHD4 and ALR amounts in cultured mammalian cells and mouse tissues. We thereby demonstrate that the redox state of the active site of CHCHD4 is partially reduced similarly to its yeast homolog. In vivo, the redox state of CHCHD4 but also the stoichiometry with its partner ALR differ between different tissues. Notably, although ALR is present in superstoichiometric ratios over CHCHD4 in almost all tissues, it does not seem to be sufficient to maintain CHCHD4 in a completely oxidized state implying diverse and partially independent functions of both proteins.

2. Results and discussion

2.1. The redox state of CHCHD4 is semioxidized in tissue culture cells

The major determinant for the proper function of CHCHD4 as an oxidoreductase is the redox state of its active site cysteines C53 and C55. The redox state of human CHCHD4 in intact cells and in vivo has not been investigated so far.

Human CHCHD4 exists in two isoforms which contain seven (isoform 1) or six cysteines (isoform 2), respectively (Fig. 1A and [9]). Four of these cysteines are in a so called structural twin CX_9C motif, while two cysteines are in the redox-active CPC motif (C53, C55) [25]. Isoform 1 contains an additional cysteine at position 4 (C4),while isoform 2 is slightly longer (155 aa vs 142 aa). Both isoforms are ubiquitously expressed on mRNA level in different tissues [9], and the presence of an additional cysteine in the N-terminal region of CHCHD4s of various species is conserved. In HEK293 cells, it appears that only isoform 1 is expressed on protein level, and we thus could limit our interpretations to this isoform with seven cysteines (Fig. S1).

In vitro, the reduction potential of the CHCHD4 redox-active CPC motif has been determined to be − 200 mV [25]. The reduction potentials of its structural disulfides are not known. However, the reduction potentials of the structural disulfides in other members of the twin CX_9C family of proteins are characterized by very low reduction potentials (< −300 mV) [26,27]. Thus, we expected that the twin CX_9C motif contains two stable, hard-to-reduce disulfide bonds, while the remaining cysteines in CHCHD4 should be easily reducible with minute amounts of reductants. To test this, we first investigated the accessibility of CHCHD4 cysteines to thiol-modifying agents upon treatment with reducing agents (Fig. 1A). To this end, we treated lysates of HEK293 cells with the reductant tris(2-carboxyethyl)phosphine (TCEP) at 4 °C and 96 °C and subsequently modified free (i.e. reduced) cysteines with the alkylating compound methyl-PEG-12-maleimide (mmPEG12) which covalently modifies free thiols and thereby slows the migration of modified proteins on SDS-PAGE. We thereby found that reduction at 4 °C only led to a small change in migration on SDS-PAGE compared to unmodified CHCHD4, which likely corresponds to modification of the reduced CPC motif, and C4 of CHCHD4. Conversely,

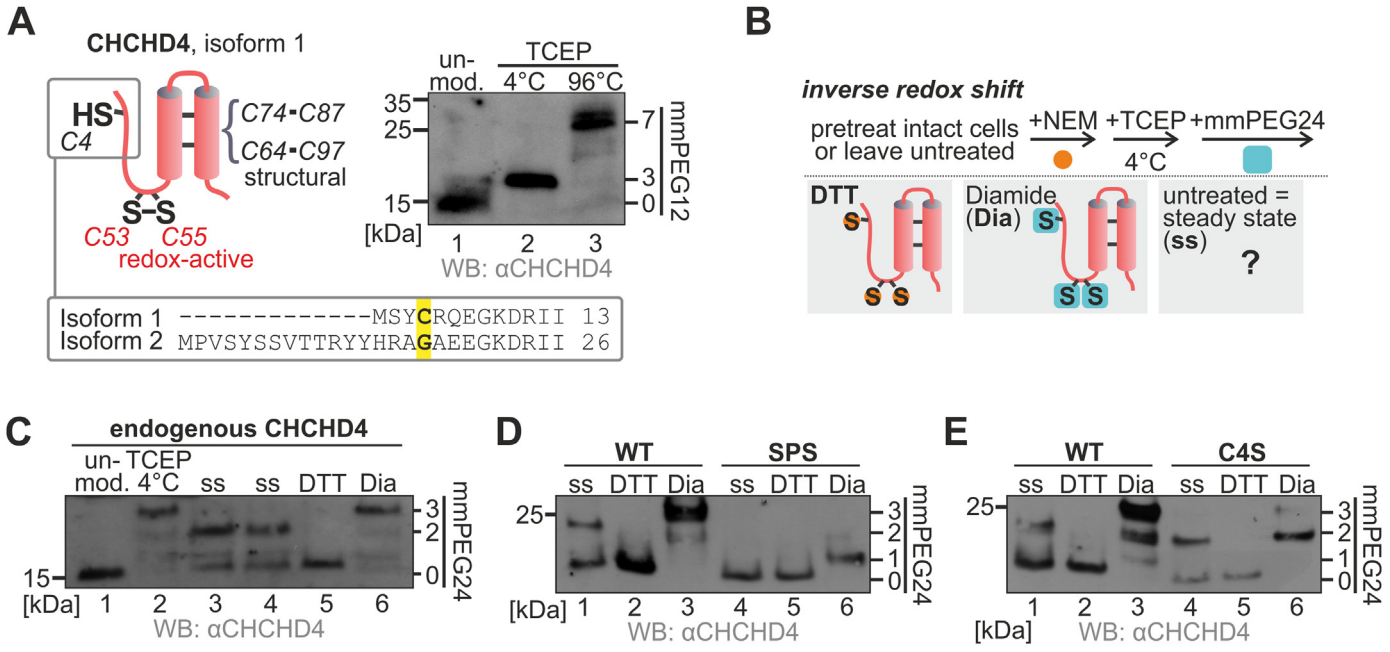

Fig. 1. The active-site cysteines in human CHCHD4 are mainly oxidized in intact cells. (A) *The layout of human CHCHD4.* Isoform 1 of CHCHD4 contains seven cysteines four of which are found in two disulfides in the structural CX_9C motif of CHCHD4. Two more are present in the redox-active CPC motif (C53/C55) and one additional is present at the N-terminus of CHCHD4 (C4, only in isoform 1). The structural disulfides in CHCHD4 are stable against treatment with the reductant TCEP at low temperature. To determine stability cell lysates were treated with TCEP at 4 °C or 96 °C and subsequently modified with mmPEG12. (B) *Layout of inverse redox state experiment.* To determine the redox state of CHCHD4 at steady state, intact cells were treated with NEM to stop all thiol-disulfide exchange reactions and trap the redox state of CHCHD4. Then, cells were lysed and lysates were treated at 4 °C with TCEP. Previously oxidized cysteines in the CPC motif are now accessible to modification with mmPEG24. As controls for the oxidized or reduced CPC motif, intact cells were treated with the oxidant diamide or the reductant DTT, respectively. As further controls, unmodified samples and samples without NEM pretreatment were loaded (not shown in the scheme). (C-E) *Redox state determination of endogenous CHCHD4 and CHCHD4 cysteine variants.* The experiment was performed as indicated in (B). HEK293 cells (C) and HEK293 cell lines stably expressing different variants of CHCHD4 (D, E) were used. The CPC motif of endogenous CHCHD4 is mainly oxidized, while C4 is reduced. Overexpression of CHCHD4 results in a slightly more reduced redox state and absence of C4 results in a more oxidized redox state of the CPC motif. The redox state experiment for endogenous CHCHD4 in HEK293 cells was performed 32 times (see Fig. 2D for quantification).

reduction at 96 °C led to a large shift indicating modification of all cysteines in CHCHD4 (Fig. 1A).

The specific behavior of the structural and redox-active cysteines in CHCHD4 enabled us to devise an approach in which we only analyzed the CPC motif and C4 of CHCHD4 (Fig. 1B, *inverse redox shift*). The stable structural disulfides remain intact, and are thus excluded from analysis. In this approach, we first blocked free cysteines in intact cells using the membrane permeable compound N-ethylmaleimide (NEM). We then lysed cells, treated the lysate at 4 °C with TCEP to reduce the previously oxidized CPC motif (and not the structural disulfide bonds) and then added mmPEG24. Using this approach, cysteines that are present in their oxidized form in intact cells become modified by mmPEG24 and consequently gain additional weight (Fig. 1C, compare lanes 5 and 6, reduced vs oxidized control). When we applied this approach to HEK293 cells we found that the redox state of endogenous CHCHD4 is characterized by the presence of two bands (Fig. 1C, lanes 3 and 4) – one that migrated at the height of the dithiothreitol (DTT)-treated control indicating a reduced CPC motif and the presence of a reduced C4. A second band migrated slightly faster than the fully oxidized control (compare with Fig. 1C, lane 6). It is likely that the latter corresponds to CHCHD4 with an oxidized CPC motif and a reduced cysteine 4, it might however also correspond to the inverse situation. To distinguish between these options we analyzed redox states of different CHCHD4 isoform 1 cysteine variants (Fig. 1D and E). Overexpressed CHCHD4 wild type in principle exhibited a similar band pattern compared to endogenous CHCHD4 but appeared to be more reduced (compare Figs. 1C and 1D,E). Analyses of the two CHCHD4 cysteine mutant variants demonstrated that C4 was present in its reduced form (Fig. 1D, lane 4). In the absence of C4 the redox-active CPC motif caused a migration pattern of CHCHD4 in two bands which was very similar to the wild type protein, although it appeared to be more oxidized compared to the wildtype situation (Fig. 1E, compare lanes 4 and 1). Thus, we can conclude that the two bands observed with endogenous CHCHD4 correspond to the reduced and oxidized redox state of the CPC motif, and that endogenous CHCHD4 is present in a predominantly oxidized form.

To verify this result we next turned to a *direct shift* approach (Fig. S2). In this approach, we stop all thiol-disulfide exchange reaction by rapid acidification using trichloroacetic acid (TCA). Concomitantly, proteins are precipitated. We then resuspended them using a buffer containing mmPEG12. Using this approach, cysteines that are present in their reduced form in intact cells become modified by mmPEG12 and consequently gain additional weight (Fig. S2, compare lanes 1,2 and 3). When we applied this approach to HEK293 cells, we found that the redox state of endogenous CHCHD4 is again characterized by the presence of two bands (Fig. S2B, lane 4) like for the inverse approach. In further orthogonal approaches, we employed alkylating agents with a different thiol modification chemistry (iodoacetyl-PEG-2-biotin, Fig. S2C) as well as radioactive labeling-based approaches (Fig. S2D, E) and found in all cases very similar semi-oxidized CHCHD4 redox states. Quantification of all redox state experiments indicated a steady state redox state of the CPC motif of about 75% oxidized and 25% reduced, and a fully reduced C4. This redox state can be modulated by ALR depletion and shift to low oxygen tensions (Fig. S3) in line with similar findings in yeast cells [21].

2.2. The redox state of CHCHD4 is semi-oxidized in vivo and varies between mouse tissues

After assigning the CHCHD4 band pattern to the oxidation state of its cysteines and determining the CHCHD4 redox state in tissue culture cells, we turned to mice to assess the CHCHD4 redox state in vivo. Notably, *Mus musculus* only contains one isoform of CHCHD4 that corresponds to isoform 1 of its human homolog (Fig. 2A). We first developed a method to preserve in vivo redox states in mice (Fig. 2B). We performed whole body NEM perfusion followed by organ harvesting. Harvested organs were then incubated in NEM for additional blocking before being snap-frozen and stored at − 80 °C. Organs were homogenized in presence of NEM, and proteins precipitated with TCA to remove excess NEM. We then determined the CHCHD4 redox state using our established *inverse redox shift* method (i.e. TCEP reduction at 4 °C as the first step, and subsequent modification with mmPEG24). As a control, we left out the TCEP incubation step. Under these conditions, no mmPEG24 modification should take place, which would indicate complete immersion of the tissues with NEM. In a second control, we left out mmPEG24 treatment to indicate “unmodified migration” of CHCHD4.

We compared the redox state of CHCHD4 in seven different tissues of three different mice. In most tissues, CHCHD4 was present mainly in the oxidized state, which is similar to the situation in tissue culture HEK293 cells (Fig. 2C). Our controls indicated full immersion of the tissues with NEM indicating that we do indeed measure in vivo redox states. We found some significant heterogeneity regarding the degree of CHCHD4 oxidation, for example in tissues like liver, CHCHD4 was about 70% oxidized, while in others like lung, skeletal muscle (a mixture of soleus/gastrocnemius) and heart the redox state was at about 90% oxidized (Fig. 2D). Thus, the CHCHD4 redox state varies significantly between tissues, which might indicate different mechanisms to maintain it, different rates of substrate import, different ratios between CHCHD4 and ALR, or additional tissue-specific functions of CHCHD4, for example acting as isomerase or reductase.

2.3. In most tissues, ALR is superstoichiometric over CHCHD4

Differences in the CHCHD4 redox state might in part be explained by differences in the stoichiometry between ALR and CHCHD4. To determine the precise molecular stoichiometry between CHCHD4 and ALR we first heterologously expressed and purified ALR and CHCHD4, confirmed that the employed amounts of CHCHD4 and ALR were in the linear range of immunoblot detection, and determined protein amounts in HEK293 cells as well as in liver and brain (Fig. 3). From these amounts, we calculated the molar ratios of ALR and CHCHD4, and thereby found that in HEK293 cells CHCHD4 was present at two-fold excess over ALR. Conversely, in liver and brain ALR was superstoichiometric over CHCHD4.

We next assessed nine different mouse tissues (Fig. 4A). Both ALR and CHCHD4 are ubiquitously expressed in mouse tissues. Notably, the ratio between both proteins strongly differed. We calculated the molar ratio between CHCHD4 and ALR (using data from Fig. 3 and S4) and confirmed that ALR is present in excess over CHCHD4 in almost all tissues with the highest ratio in liver, heart and skeletal muscle (Fig. 4B). This is very different from yeast mitochondria where Mia40 is in large excess over Erv1 [28].

In vitro, ALR can catalyze fast reoxidation of CHCHD4 even at low substoichiometric levels. An excess of ALR over CHCHD4 in vivo thus makes it likely that ALR fulfills additional roles than just CHCHD4 reoxidation. This is supported further by the fact that the ratio of CHCHD4 and ALR does only correlate weakly with the redox states of CHCHD4 in different tissues (Fig. S4C). Likewise, CHCHD4 levels also only correlate weakly with the redox state (Fig. S4D).

2.4. Conclusion - in vivo insights into the mammalian mitochondrial disulfide relay

Components of the mammalian disulfide relay machinery have mainly been characterized in vitro as purified proteins. Yet, the mammalian disulfide relay has been linked to many crucial cellular functions in and outside of mitochondria that cannot merely be understood by in vitro approaches [9,10,29,30]. In this study, we explored the importance of the redox-active cysteines in CHCHD4 with respect to their redox state in vivo. We thereby found that in mammalian cells, the CHCHD4 redox state is mainly oxidized however with significant

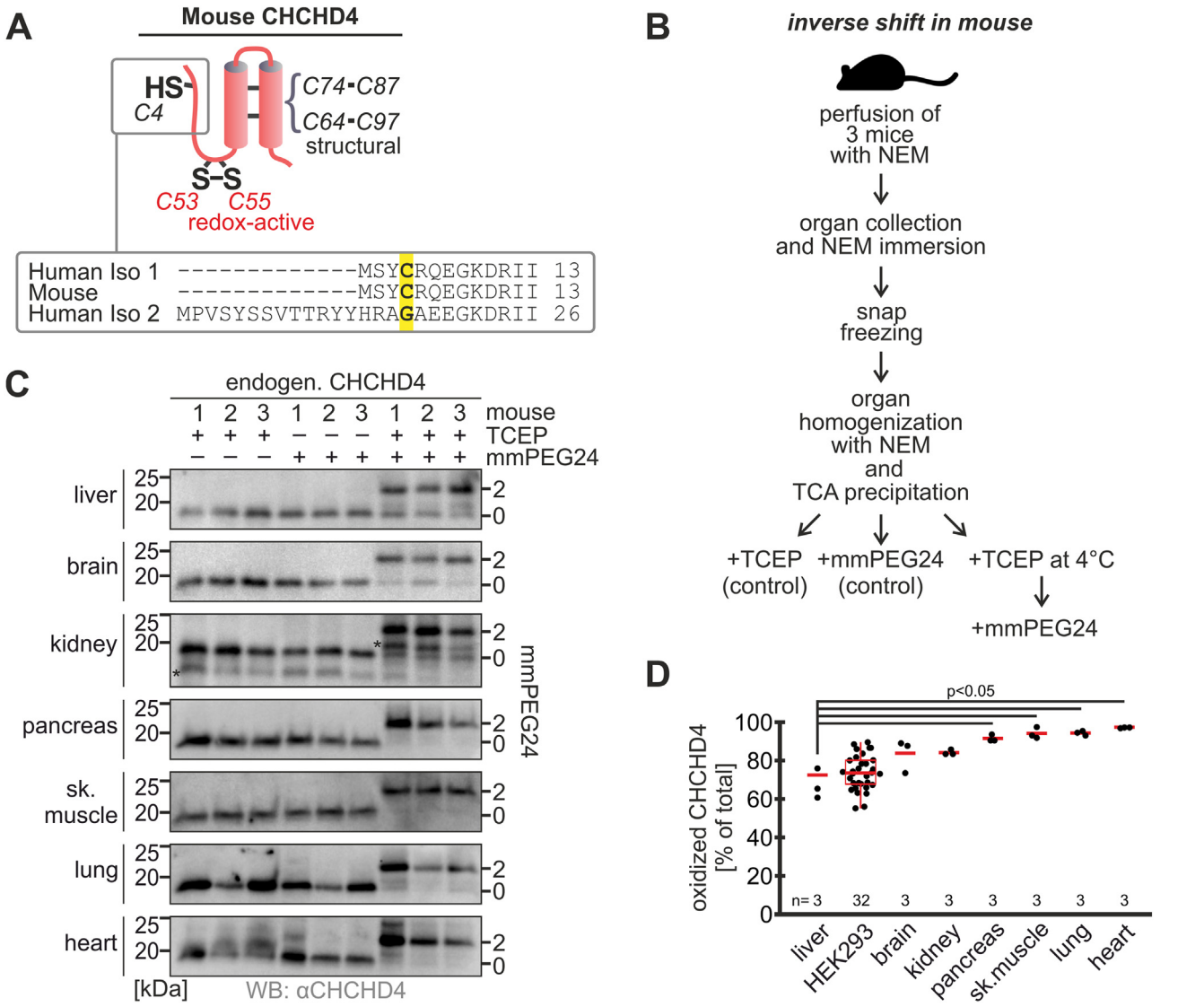

Fig. 2. The redox state of the CHCHD4 active site is mainly oxidized and shows differences between mouse tissues. (A) *The layout of mouse CHCHD4.* Mouse CHCHD4 is present as one isoform only, which corresponds to isoform 1 of human CHCHD4. Mouse CHCHD4 also contains C4. (B) *Layout of in vivo redox state experiment.* To determine the in vivo redox state of CHCHD4 at steady state, mice were perfused with NEM-containing buffer (PBS-NEM), organs extracted and incubated again in PBS-NEM and then snap-frozen. Organs were homogenized in presence of NEM, and lysates TCA precipitated to remove any excess NEM. Lysates were treated at 4 °C with TCEP, modified with mmPEG24 and analyzed by immunoblot against CHCHD4. As controls, samples were only treated with either TCEP or mmPEG24. (C) *CHCHD4 redox states in different mouse organs.* The experiment was performed as described in (A) with three different mice (n = 3). Asterisk shows cross-reaction bands. (D) *Quantification of CHCHD4 redox states.* Results from (B) were quantified and compared to the redox state of CHCHD4 in HEK293 cells (n = 32). The CHCHD4 redox states differ between different tissues. Black dot represents the value from each experiment; red line represents the mean value. Statistical analysis was performed with one-way ANOVA followed by Tukey's post-analysis. Statistical significance was indicated where present.

differences between different mouse tissues. Importantly, while ALR in vitro is a very efficient catalyst of CHCHD4 reoxidation, its super-stoichiometric presence in almost all tissues appears not to be sufficient to oxidize CHCHD4 fully. Potential explanations might be that a pool of ALR never encounters CHCHD4, that a pool of ALR is kept inactive much like its ER counterpart Ero1, that there are different oxygen tensions and different substrate loads in mitochondria of different tissues or that CHCHD4 and/or ALR fulfil functions independently from each other that are different from IMS protein import. The differences in CHCHD4 redox state might also provide a mechanistic explanation why patient mutations in CHCHD4 substrates show strong tissue differences [16,31] and highlight the importance of tissue specific analyses of mitochondrial import and biogenesis pathways.

3. Material and methods

3.1. Plasmids, cell lines, siRNAs, and antibodies

For plasmids, cell lines, and primers used in this study, see Supplemental Tables S1 and S2. For the generation of stable, inducible cell lines the HEK293 cell line–based Flp-In™ T-REx™ – 293 cell line was used with the Flp-In™ T-REx™ system (Invitrogen, Carlsbad, VA). The following siRNAs were used: Hs_GFER_1, Hs_GFER_6, control siRNA (Quiagen). Hs_CHCHD4_5 (UTR-1/2c), Hs_CHCHD4_6 (UTR-1/2d) (Quiagen), CHCHD4-CDS-1/2a (ATGTCCTATTGCCGGCAGGAAGTT), CHCHD4-CDS-1/2b (GATCGAATCATATTTGTAA), CHCHD4-CDS-2 (CTGTGACCACCAGGTACTA) (Sigma-Aldrich). Antibodies: anti-ALR (self-made), anti-CHCHD4 (self-made; [14]), anti-CHCHD4 (Sigma, HPA034688), anti-AIF (Santa Cruz Biotechnology, sc-5586), anti-cytochrome *c* (Cell Signaling Technology, Cat#4272, RRID:AB_2090454),

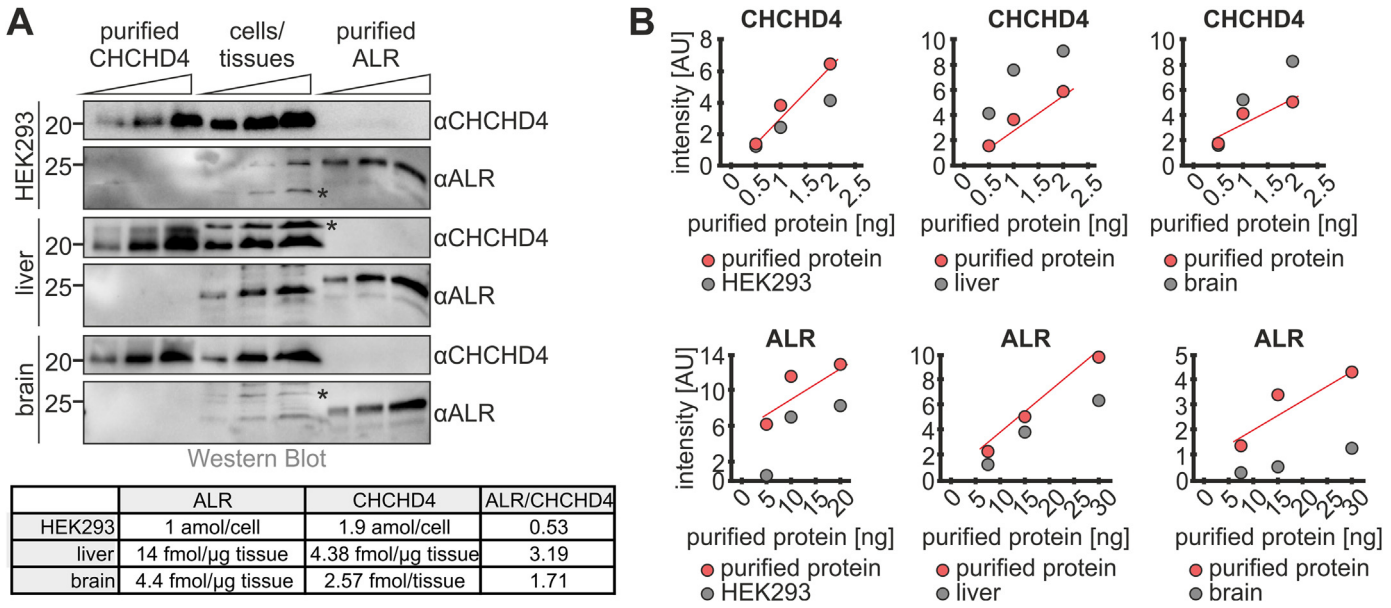

	ALR	CHCHD4	ALR/CHCHD4
HEK293	1 amol/cell	1.9 amol/cell	0.53
liver	14 fmol/µg tissue	4.38 fmol/µg tissue	3.19
brain	4.4 fmol/µg tissue	2.57 fmol/tissue	1.71

Fig. 3. Determination of ALR and CHCHD4 amounts in cells and mouse tissues. (A) Human ALR and human CHCHD4 were expressed heterologously and purified from *E. coli*. CHCHD4 protein was loaded 0.5–1–2 ng per well, respectively. ALR protein was loaded 5–10–20 ng or 7.5–15–30 ng per well, respectively. Cell amounts were 5–10–20 × 10^4 and tissue amounts were 15, 30 and 60 µg per well, respectively. The quantification of blots was performed using Bio-Rad Image Lab software. Of note, the molecular weight of human ALR is about 0.6 kDa higher compared to mouse ALR. In addition, purified ALR still contains a short linker fragment of about 0.4 kDa. The experiments were performed two times. (B) Values are plotted and indicate that signal intensities for purified proteins is in a similar range as signal intensities for CHCHD4 and ALR in cells/tissues. Molar amounts of CHCHD4 and ALR per cell or per µg tissue protein were calculated comparing the signals. From these values, molar ratios of ALR over CHCHD4 were calculated (see table). Asterisk shows cross-reaction bands.

anti-HIF1α (Cell Signaling Technology Cat# 3716, RRID:AB_2116962), anti-Oxphos (MitoScience LLC Cat# MS601, RRID:AB_478275; only COXII is shown in Fig. 4), anti-PDH (Santa Cruz Biotechnology, Cat# sc-377092), anti-SOD1 (Biomol, Cat# S8060–12 J)

3.2. Assay to address inverse and direct redox states of protein thiols

For *inverse* shifts in which the reduced thiols were initially blocked, cells were treated with 15 mM NEM (N-Ethylmaleimide) dissolved in PBS at 4 °C for 15 min. Reduced controls were pretreated with 10 mM DTT (Dithiothreitol) and oxidized controls were pretreated with 10 mM

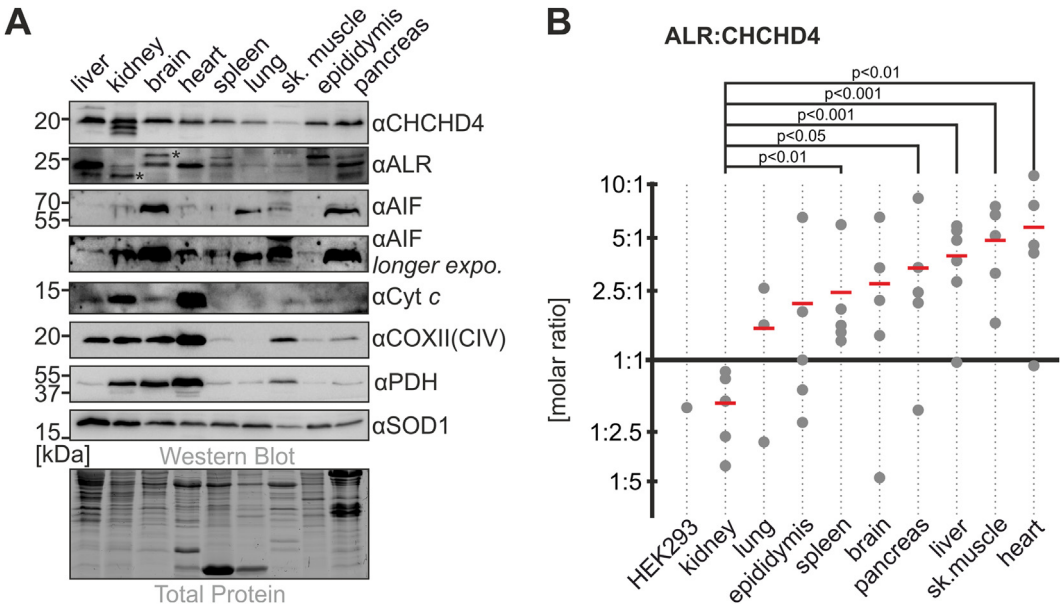

Fig. 4. Determination of the molar ratio of ALR over CHCHD4 in cells and mouse tissues. (A) *Levels of CHCHD4, ALR and indicated proteins in several mouse tissues*. After organ lysis and homogenization, protein amounts were quantified and equal amounts proteins (40 µg/lane) were loaded and analyzed using the indicated antibodies. CHCHD4 and ALR are ubiquitous with varying amounts in different tissues. In Figs. 3 and 4 the same samples were used for HEK293 cells, liver and brain. (B) Using the quantification of CHCHD4 and ALR amounts from three to five different mice (comparing signal intensities of purified protein amounts and tissues to obtain absolute values of CHCHD4 and ALR from experiments in Figs. 3A, 4A and S4), the molar ratio of ALR over CHCHD4 were calculated for HEK293 cells and the mouse tissues. Gray dots represent the value from each mouse experiment; red lines represent the mean values. Statistical analysis was performed with one-way ANOVA followed by Tukey's post-analysis. Statistical significance was indicated where present.

Diamide in the culture medium for 10 min, and afterwards blocked with NEM. For *direct* shifts, the cells were only washed with PBS. Thiol-exchange reactions were frozen in the cells by addition of 8% ice cold TCA. TCA precipitation of proteins was performed by centrifugation at 13,000 ×*g* for 15 min and washing with 5% TCA. Protein precipitates were dissolved in 40 µl of modification buffer (0.2 M Tris, pH 7.5, 6 M urea, 10 mM EDTA, 2% SDS) by sonication and treated with 5 mM TCEP (Tris(2-carboxyethyl)phosphine) for 15 min at 4 °C before mmPEG24 modification (15 µM final concentration). As controls, indicated samples were only treated with TCEP or mmPEG24. After modification samples were filled to 100 µl with ddH_2O and Laemmli buffer (2% SDS, 60 mM Tris, pH 6.8, 10% glycerol, 0.0025% bromphenol blue) and 10 µl of sample was loaded and separated on SDS-PAGE, analyzed by Western Blotting and immunodetection.

3.3. NEM perfusion of mice for the assessment of CHCHD4 redox state in vivo

Animal experiments were conducted according to local, national, and European Union ethical guidelines and approved by local regulatory authorities. Animal license number: 08–2017.

Male C57Bl6/N mice were anesthetized by injection of mixed solution of ketamine (1.4%) and xylazine (0.2%; ml/kg body weight), and intra-cardially perfused with 50 mM NEM in 0.1 M phosphate buffer (pH 7.4) for 10 min, perfusion rate 5 ml/min. After perfusion, organs were harvested and kept in 50 mM NEM solution for an additional 5 min, before being snap-frozen. The frozen organs were stored at − 80 °C.

For generating a lysate, the tissue was soaked in 3 ml of RIPA buffer (150 mM NaCl, 50 mM Tris–HCl pH 7.4, 5 mM EDTA, 1% Triton X-100, 1% sodium deoxycholate, 0.1% SDS) supplemented with 15 mM NEM per gram of tissue and cut into small pieces with scissors in a reaction tube. The tissue was homogenized in the reaction tube using a handheld potter homogenizer. The liquefied tissue was centrifuged at 10,000 ×g for 10 min at 4 °C. The cleared supernatant was transferred into a new reaction tube and protein amount was determined using BCA assay. The protein amount was adjusted to 5 µg/µl by addition of RIPA buffer and the lysate was aliquoted, snap frozen in liquid nitrogen. For redox state determination, 150 µg of tissue lysate was precipitated in 1 ml of 8% TCA and the further treatment was performed after resolving the precipitate in buffer A as described in the inverse redox shift assay.

3.4. Heterologous protein expression and purification

The protein expressions and purifications of human CHCHD4 and human ALR was essentially performed as described in [32] for the yeast proteins. The concentration of the purified protein was determined using BCA assay and was subsequently validated using SDS-PAGE and TCA staining by BSA calibration.

3.5. Quantification and statistics

Western blots detections were performed using ECL reagents (ECL-1: 100 mM Tris pH 8.5, 0.044% (w/v) luminol, 0.0066% p-Coumaric acid; ECL-2: 100 mM Tris pH 8.5, 0.2% H_2O_2). Luminescence was detected for some experiments on X-ray films (Fuji Medical X-Ray Film Super RX). In this case, the films were digitally scanned and signals in the linear detection range were quantified using ImageJ software. Luminescence was digitally detected for some experiments using Bio-Rad ChemiDoc™ Touch and signals in the linear detection range were quantified using Bio-Rad Image Lab software. Statistical analysis was performed with one-way ANOVA followed by Tukey's post-analysis. p values below 0.05 were considered to indicate statistical significance.

Acknowledgments

Research in the author's laboratory is funded by the German research council to JR (DFG, (RI2150/1–2, RI2150/2-2 and SFB1218/TP B02)). MH received a PhD scholarship from the *Carl Zeiss foundation*, and CP from the *Boehringer Ingelheim Fonds*. LWT was funded by MRC grants (MR/K002201/1 and MR/K002201/2) to MA. We thank Anja Wittmann for technical help, and Bruce Morgan (Kaiserslautern) for critically reading the manuscript.

Author contribution

MA, AE, MH, SS, LS, and CP planned and performed experiments. LPR performed NEM perfusions of mice. MA and LWT cloned CHCHD4-myc constructs. LIL helped with proteomic experiments. All authors discussed and analyzed the data. AE, MH and JR wrote the manuscript. JR designed and planned the study.

Author disclosure statement

No competing financial interests and conflicts of interest exist.

Appendix A. Supplementary material

Supplementary data associated with this article can be found in the online version at http://dx.doi.org/10.1016/j.redox.2018.03.014.

References

[1] E. Hangen, et al., Interaction between AIF and CHCHD4 regulates respiratory chain biogenesis, Mol. Cell 58 (6) (2015) 1001–1014.
[2] T. Lisowsky, Dual function of a new nuclear gene for oxidative phosphorylation and vegetative growth in yeast, Mol. Gen. Genet 232 (1) (1992) 58–64.
[3] A. Chacinska, et al., Essential role of Mia40 in import and assembly of mitochondrial intermembrane space proteins, EMBO J. 23 (19) (2004) 3735–3746.
[4] J. Riemer, N. Bulleid, J.M. Herrmann, Disulfide formation in the ER and mitochondria: two solutions to a common process, Science 324 (5932) (2009) 1284–1287.
[5] D. Stojanovski, P. Bragoszewski, A. Chacinska, The MIA pathway: a tight bond between protein transport and oxidative folding in mitochondria, Biochim Biophys. Acta 1823 (7) (2012) 1142–1150.
[6] N. Modjtahedi, et al., Mitochondrial proteins containing coiled-coil-helix-coiled-coil-helix (CHCH) domains in health and disease, Trends Biochem Sci. 41 (3) (2016) 245–260.
[7] C. Petrungaro, et al., The Ca(2+)-dependent release of the Mia40-induced MICU1-MICU2 dimer from MCU regulates mitochondrial Ca(2+) uptake, Cell Metab. 22 (4) (2015) 721–733.
[8] L.W. Thomas, et al., CHCHD4 regulates intracellular oxygenation and perinuclear distribution of mitochondria, Front Oncol. 7 (2017) 71.
[9] J. Yang, et al., Human CHCHD4 mitochondrial proteins regulate cellular oxygen consumption rate and metabolism and provide a critical role in hypoxia signaling and tumor progression, J. Clin. Invest 122 (2) (2012) 600–611.
[10] J. Zhuang, et al., Mitochondrial disulfide relay mediates translocation of p53 and partitions its subcellular activity, Proc. Natl. Acad. Sci. USA 110 (43) (2013) 17356–17361.
[11] R. Pawlowski, J. Jura, ALR and liver regeneration, Mol. Cell Biochem 288 (1–2) (2006) 159–169.
[12] T. Endo, K. Yamano, S. Kawano, Structural basis for the disulfide relay system in the mitochondrial intermembrane space, Antioxid. Redox Signal 13 (9) (2010) 1359–1373.
[13] P. Manganas, L. MacPherson, K. Tokatlidis, Oxidative protein biogenesis and redox regulation in the mitochondrial intermembrane space, Cell Tissue Res 367 (1) (2017) 43–57.
[14] M. Fischer, et al., Protein import and oxidative folding in the mitochondrial intermembrane space of intact mammalian cells, Mol. Biol. Cell 24 (14) (2013) 2160–2170.
[15] S. Hofmann, et al., Functional and mutational characterization of human MIA40 acting during import into the mitochondrial intermembrane space, J. Mol. Biol. 353 (3) (2005) 517–528.
[16] M.W. Friederich, et al., Mutations in the accessory subunit NDUFB10 result in isolated complex I deficiency and illustrate the critical role of intermembrane space import for complex I holoenzyme assembly, Hum. Mol. Genet 26 (4) (2017) 702–716.
[17] S.R. Farrell, C. Thorpe, Augmenter of liver regeneration: a flavin-dependent sulfhydryl oxidase with cytochrome c reductase activity, Biochemistry 44 (5) (2005) 1532–1541.
[18] K. Bihlmaier, et al., The disulfide relay system of mitochondria is connected to the

respiratory chain, J. Cell Biol. 179 (3) (2007) 389–395.
[19] M.E. Sztolsztener, et al., Disulfide bond formation: sulfhydryl oxidase ALR controls mitochondrial biogenesis of human MIA40, Traffic 14 (3) (2013) 309–320.
[20] A. Di Fonzo, et al., The mitochondrial disulfide relay system protein GFER is mutated in autosomal-recessive myopathy with cataract and combined respiratory-chain deficiency, Am. J. Hum. Genet 84 (5) (2009) 594–604.
[21] K. Kojer, et al., Glutathione redox potential in the mitochondrial intermembrane space is linked to the cytosol and impacts the Mia40 redox state, EMBO J. 31 (14) (2012) 3169–3182.
[22] K. Kojer, et al., Kinetic control by limiting glutaredoxin amounts enables thiol oxidation in the reducing mitochondrial intermembrane space, Mol. Biol. Cell 26 (2) (2015) 195–204.
[23] J.R. Koch, F.X. Schmid, Mia40 combines thiol oxidase and disulfide isomerase activity to efficiently catalyze oxidative folding in mitochondria, J. Mol. Biol. 426 (24) (2014) 4087–4098.
[24] D.A. Hudson, C. Thorpe, Mia40 is a facile oxidant of unfolded reduced proteins but shows minimal isomerase activity, Arch. Biochem Biophys. 579 (2015) 1–7.
[25] L. Banci, et al., MIA40 is an oxidoreductase that catalyzes oxidative protein folding in mitochondria, Nat. Struct. Mol. Biol. 16 (2) (2009) 198–206.
[26] A. Voronova, et al., Oxidative switches in functioning of mammalian copper chaperone Cox17, Biochem J. 408 (1) (2007) 139–148.
[27] H. Lu, J. Woodburn, Zinc binding stabilizes mitochondrial Tim10 in a reduced and import-competent state kinetically, J. Mol. Biol. 353 (4) (2005) 897–910.
[28] L. Banci, et al., Molecular recognition and substrate mimicry drive the electron-transfer process between MIA40 and ALR, Proc. Natl. Acad. Sci. USA 108 (12) (2011) 4811–4816.
[29] L.R. Todd, et al., Growth factor erv1-like modulates Drp1 to preserve mitochondrial dynamics and function in mouse embryonic stem cells, Mol. Biol. Cell 21 (7) (2010) 1225–1236.
[30] J. Zhuang, et al., Forkhead Box O3A (FOXO3) and the mitochondrial disulfide relay carrier (CHCHD4) regulate p53 protein nuclear activity in response to exercise, J. Biol. Chem. 291 (48) (2016) 24819–24827.
[31] L. Tranebjaerg, et al., A de novo missense mutation in a critical domain of the X-linked DDP gene causes the typical deafness-dystonia-optic atrophy syndrome, Eur. J. Hum. Genet 8 (6) (2000) 464–467.
[32] M. Bien, et al., Mitochondrial disulfide bond formation is driven by intersubunit electron transfer in Erv1 and proofread by glutathione, Mol. Cell 37 (4) (2010) 516–528.